

# Targeting a thrombopoietin-independent strategy in the discovery of a novel inducer of megakaryocytopoiesis, DMAG, for the treatment of thrombocytopenia

Long Wang,<sup>1\*</sup> Sha Liu,<sup>2\*</sup> Jiesi Luo,<sup>1\*</sup> Qi Mo,<sup>1</sup> Mei Ran,<sup>1</sup> Ting Zhang,<sup>1</sup> Xiaoxuan Li,<sup>1</sup> Wenjun Zou,<sup>3</sup> Qibing Mei,<sup>1</sup> Jianping Chen,<sup>4</sup> Jing Yang,<sup>5</sup> Jing Zeng,<sup>1</sup> Feihong Huang,<sup>1</sup> Anguo Wu,<sup>1</sup> Chunxiang Zhang<sup>6</sup> and Jianming Wu<sup>7,1,6</sup>

<sup>1</sup>Department of Pharmacology, School of Pharmacy, Southwest Medical University, Luzhou, Sichuan; <sup>2</sup>Department of Gastroenterology, The Affiliated Hospital of Southwest Medical University, Luzhou, Sichuan; <sup>3</sup>School of Pharmacy, Chengdu University of Traditional Chinese Medicine, Chengdu, Sichuan; <sup>4</sup>School of Chinese Medicine, The University of Hong Kong, Hong Kong; <sup>5</sup>Department of Pharmacy, Chengdu Fifth People's Hospital, Chengdu University of Traditional Chinese Medicine, Chengdu, Sichuan; <sup>6</sup>Education Ministry Key Laboratory of Medical Electrophysiology, Sichuan Key Medical Laboratory of New Drug Discovery and Druggability Evaluation, Luzhou Key Laboratory of Activity Screening and Druggability Evaluation for Chinese Materia Medica, Southwest Medical University, Luzhou, Sichuan and <sup>7</sup>School of Basic Medical Sciences, Southwest Medical University, Luzhou, Sichuan, China

\*LW, SL and JL contributed equally to this work as co-first authors.

**Correspondence:** W. Jianming  
[jianmingwu@swmu.edu.cn](mailto:jianmingwu@swmu.edu.cn)  
 Z.Chunxiang  
[zhangchx999@163.com](mailto:zhangchx999@163.com)  
 W.Anguo  
[wag1114@foxmail.com](mailto:wag1114@foxmail.com)

**Received:** October 1, 2022.  
**Accepted:** December 15, 2022.  
**Early view:** December 22, 2022.

<https://doi.org/10.3324/haematol.2022.282209>

©2023 Ferrata Storti Foundation

Published under a CC BY-NC license



## Abstract

Thrombocytopenia is a thrombopoietin (TPO)-related disorder with very limited treatment options, and can be life-threatening. There are major problems with typical thrombopoietic agents targeting TPO signaling, so it is urgent to discover a novel TPO-independent mechanism involving thrombopoiesis and potential druggable targets. We developed a drug screening model by the multi-grained cascade forest (gcForest) algorithm and found that 3,8-di-O-methylellagic acid 2-O-glucoside (DMAG) (10, 20 and 40  $\mu\text{M}$ ) promoted megakaryocyte differentiation *in vitro*. Subsequent investigations revealed that DMAG (40  $\mu\text{M}$ ) activated ERK1/2, HIF-1 $\beta$  and NF-E2. Inhibition of ERK1/2 blocked megakaryocyte differentiation and attenuated the upregulation of HIF-1 $\beta$  and NF-E2 induced by DMAG. Megakaryocyte differentiation induced by DMAG was inhibited via knockdown of NF-E2. *In vivo* studies showed that DMAG (5 mg/kg) accelerated platelet recovery and megakaryocyte differentiation in mice with thrombocytopenia. The platelet count of the DMAG-treated group recovered to almost 72% and 96% of the count in the control group at day 10 and 14, respectively. The platelet counts in the DMAG-treated group were almost 1.5- and 1.3-fold higher compared with those of the irradiated group at day 10 and 14, respectively. Moreover, DMAG (10, 25 and 50  $\mu\text{M}$ ) stimulated thrombopoiesis in zebrafish. DMAG (5 mg/kg) could also increase platelet levels in c-MPL knockout (c-MPL<sup>-/-</sup>) mice. In summary, we established a drug screening model through gcForest and demonstrated that DMAG promotes megakaryocyte differentiation via the ERK/HIF1/NF-E2 pathway which, importantly, is independent of the classical TPO/c-MPL pathway. The present study may provide new insights into drug discovery for thrombopoiesis and TPO-independent regulation of thrombopoiesis, as well as a promising avenue for thrombocytopenia treatment.

## Introduction

Platelets are crucial for hemostasis, thrombosis, the innate immune response, angiogenesis, inflammation and infection.<sup>1,2</sup> Platelets are produced by megakaryocytes, which are derived from hematopoietic stem cells that undergo a continuous process of hematopoietic lineage differentiation. The progress of megakaryocyte differentiation plays

an essential role in the schedule and output of platelet production.<sup>3</sup> During differentiation, megakaryocytes undergo endomitosis and cytoplasmic maturation, which results in increased ploidy, cell volume and surface area-to-volume ratio and provides an extensive membrane system for further platelet formation.<sup>3</sup> The classical TPO/c-MPL signaling pathway is a major driver of megakaryocyte differentiation. TPO (thrombopoietin) binds to its

receptor, c-MPL, which induces phosphorylation of JAK2. Subsequently, JAK2 phosphorylates many downstream substrates, leading to the activation of multiple signaling pathways, including STAT3/STAT5, PI3K/AKT and MAPK/ERK. Finally, these activated signaling pathways induce or repress the expression of several transcription factors, such as GATA1, RUNX1, NF-E2, AML1, FLI1 and TAL1, which further promote megakaryocyte differentiation and platelet formation.<sup>1,3</sup>

Thrombocytopenia, a disorder of low platelet count, is caused by a variety of factors, including radiotherapy and chemotherapy used to treat cancers or tumors. Thrombocytopenia has been a challenge in the clinic for a long time and can lead to abnormal bleeding, infection, poor prognosis and even death.<sup>3-5</sup> However, at present, there are still no approved agents for the rapid treatment of radiation- or chemotherapy-induced thrombocytopenia.<sup>5,6</sup> Generally, platelet transfusion and non-specific drugs, including cytokines, hormones and immunosuppressants, are used to treat thrombocytopenia in the clinic. However, these treatments are usually associated with several harmful side-effects that limit their clinical use.<sup>7,8</sup> Therefore, it is urgent to develop non-toxic and non-immunogenic reagents for the treatment of thrombocytopenia. At present, TPO-receptor agonists are the only effective treatment choices for patients with chronic thrombocytopenia who are unresponsive to steroids. However, these drugs may increase the risk of venous and arterial thrombosis, bone marrow (BM) fibrosis, acute myelogenous leukemia and liver toxicity.<sup>8</sup> In addition, treatment with a TPO-receptor agonist is not an applicable option for patients who are refractory to these agonists or who have a complete loss of functional c-MPL.<sup>9-11</sup> It is, therefore, imperative to develop TPO-alternative therapeutic options to manage thrombocytopenia.

At present, drug discovery still faces numerous challenges and problems, such as high cost, time consumption, off-target delivery and low efficacy. The identification of suitable, bioactive drug molecules from millions of candidate compounds is extremely difficult and a disheartening part of the drug discovery and development process.<sup>12</sup> Fortunately, with rapid advancements in computational power, the blossoming of deep learning technology and the growth of drug-related data, various deep learning-based methodologies have been successfully exploited in all steps of the drug discovery and development process, and can identify potential, active compounds in the vast realm of chemical space quickly and cheaply.<sup>13,14</sup> As a primary branch of artificial intelligence, machine learning plays a crucial role in drug discovery and development and includes random forest, support vector machine, k-nearest neighbors, naïve Bayesian, artificial neural networks, principal component analysis, and soon on.<sup>12</sup> Deep learning is an important subfield of machine learning.<sup>12</sup> Recently, a

new machine learning method, deep forest or multi-grained cascade forest (gcForest), has been proposed.<sup>15,16</sup> The gcForest algorithm is a combination of traditional machine learning algorithms and deep learning ideas, which shows a greater learning ability and estimation accuracy than any single algorithm. There is no doubt that in the near future, gcForest will provide an alternative avenue and will be in the spotlight for drug discovery.<sup>16</sup>

To discover more effective agents for use in the treatment of thrombocytopenia, we developed a drug screening model based on the gcForest algorithm to predict active compounds. We then aimed to investigate the effects of 3,8-di-O-methylellagic acid 2-O-glucoside (DMAG), a potential active compound predicted by the drug screening model, on megakaryocyte differentiation and platelet formation, and to elucidate its mechanism of action against thrombocytopenia. Our findings could provide a new therapeutic approach to thrombocytopenia.

## Methods

### Measurement of megakaryocyte differentiation

Cells incubated with DMAG (10, 20 and 40  $\mu$ M) for 6 days were harvested and labeled with FITC-CD41 and PE-CD42b antibodies (Biolegend, San Diego, CA, USA) for 30 min on ice in the dark. The percentages of CD41<sup>+</sup>CD42b<sup>+</sup> cells were evaluated by a BD FACSCanto II flow cytometer (BD Biosciences, San Jose, CA, USA).

### Animals

Specific pathogen-free Kunming (KM) mice and C57BL/6 mice (8-10 weeks old, weighing 18-22 g) were purchased from Da-suo Biotechnology Limited (Chengdu, China). Tg (cd41:eGFP) transgenic zebrafish were obtained from the Chinese National Zebrafish Resource Center (Wuhan, China). All procedures involving mice and zebrafish were performed in compliance with the laboratory animal ethics committee of Southwest Medical University (License N. 20211123-014).

### Construction of a model of carotid artery thrombosis

A ferric chloride (FeCl<sub>3</sub>)-induced model of carotid arterial thrombus was constructed as described previously.<sup>17,18</sup> Briefly, the mice were administered normal saline, TPO (3,000 U/kg), or DMAG (5 mg/kg) daily after irradiation for 10 days and then anesthetized by intraperitoneal injection of sodium pentobarbital (50 mg/kg). The common carotid arteries were exposed, and filter paper (3 × 1.0 mm) saturated with 10% (w/v) FeCl<sub>3</sub> was placed on top of the left carotid artery for 3 min to induce thrombosis. After removal of the filter paper, the carotid artery was washed with phosphate-buffered saline. The blood flow was continuously monitored with a vascular flow probe using a

Transonic Model TS420 flowmeter (Transonic Systems, Ithaca, NY, USA) from the onset of the injury until stable occlusion occurred (defined as no flow for 120 min).

### Construction of the c-MPL knockout mouse model and treatment of the mice

CRISPR/Cas9-mediated genome engineering<sup>19</sup> was used to create a c-MPL knockout (c-MPL<sup>-/-</sup>) mouse model (C57BL/6 mice). Considering that the c-MPL-201 transcript has 12 exons, we designed two gRNA targeting the 5' untranslated region and exon 12 to create a thorough knockout model. The gRNA were designed on *crispr.mit.edu*, and high-score gRNA were used. Cas9 and two gRNA were co-injected into fertilized eggs to produce the knockout mice. The pups were genotyped by polymerase chain reaction (PCR) followed by sequence analysis. The c-MPL<sup>-/-</sup> mice were randomly divided into two groups (6 males and 6 females in each group): the control group and the DMAG-treated group. The control group and DMAG-treated group were injected intraperitoneally with normal saline or DMAG (5 mg/kg), respectively, for 14 days. Venous plexus blood was collected from the mouse eyes, and routine blood tests were then performed with an automatic blood cell analyzer. The sequences of the gRNA and PCR screening primers are listed in *Online Supplementary Table S1*.

### Statistical analysis

All data are expressed as the mean  $\pm$  standard deviation from at least three independent experiments. Statistical analysis of comparisons among the multiple groups was assessed by one-way analysis of variance (ANOVA) followed by the Tukey *post-hoc* test. Differences between two groups were analyzed using two-tailed Student *t* tests. A *P* value <0.05 was considered statistically significant.

## Results

### Construction of the drug screening model based on gcForest and prediction of active compounds

Considering that traditional drug discovery in the laboratory is aimless, costly and ineffective, it would be of extreme utility to build a drug screening model for high-throughput virtual screening of potential active compounds before experimental verification. In the present study, we first developed a drug screening model through gcForest (Figure 1A). Of the six datasets, the dataset with an importance ratio of 50% showed the best prediction performance, with an area under the curve (AUC) value of 0.78 (Figure 1C). The validation set containing two active and ten inactive compounds was then used as the input into the model, and the prediction accuracy of the model was 84.6%. Finally, a chemical library was used to predict active compounds through the drug screening model. The

results showed that a natural compound, DMAG, exhibited a very high score of 0.79, indicating that DMAG might have high activity.

### DMAG dose-dependently induces megakaryocyte differentiation and maturation

The activities of the potential active compounds predicted by the model were investigated *in vitro*. Excitingly, we found that DMAG (*Online Supplementary Figure S1A*), a natural product, had excellent activity in inducing megakaryocyte differentiation of HEL and Meg-01 cells (Figure 2, *Online Supplementary Figure S2*). After treatment for 6 days, we noted the appearance of numerous large megakaryocyte-like cells in the DMAG (10, 20 and 40  $\mu$ M)-treated HEL group but not in the control HEL group (Figure 2A). Wright-Giemsa staining showed that DMAG significantly increased the cell size and the number of nuclei in HEL cells (Figure 2B). After treatment for 6 days, flow cytometry analysis showed that the expression of the megakaryocytic lineage-specific differentiation marker CD41 and maturation marker CD42b increased in a dose-dependent manner in the DMAG-treated groups (Figure 2C).

A polyploid nucleus is a typical characteristic of mature megakaryocytes. The ploidy was readily validated by DAPI and phalloidin staining in the DMAG-treated group (Figure 2D). Flow cytometry analysis also showed that DMAG markedly increased DNA ploidy in a dose-dependent manner in HEL cells (Figure 2E). A similar result was found in Meg-01 cells (*Online Supplementary Figure S2*). In addition, a lactate dehydrogenase assay was performed to detect the cytotoxicity of DMAG. The results suggested that all concentrations of DMAG (10, 20 and 40  $\mu$ M) had no cytotoxicity on HEL cells (*Online Supplementary Figure S1B*). These results demonstrate that DMAG is a safe inducer of megakaryocyte differentiation and maturation.

### Stage- and time-specific activation of ERK1/2 and HIF-1 $\beta$ is involved in DMAG-induced megakaryocyte differentiation

To investigate genomic changes related to the promoting effect of DMAG on megakaryocyte differentiation, we collected cells from the control group and DMAG (40  $\mu$ M)-treated group and performed RNA sequencing. The transcriptome results showed that a total of 4,030 mRNA were differentially expressed (fold-change >2.0 and *P*<0.05). Kyoto Encyclopedia of Genes and Genomes (KEGG) pathway analysis was applied to identify signaling pathways regulated by DMAG. The results demonstrated that the upregulated mRNA were significantly enriched in MAPK and HIF-1 signaling pathways (Figure 3A), which are closely related to megakaryocyte differentiation.<sup>1,20</sup> Conversely, the downregulated mRNA were primarily associated with metabolic, Epstein-Barr virus infection and viral carcinogenesis pathways (Figure 3B). The KEGG pathway

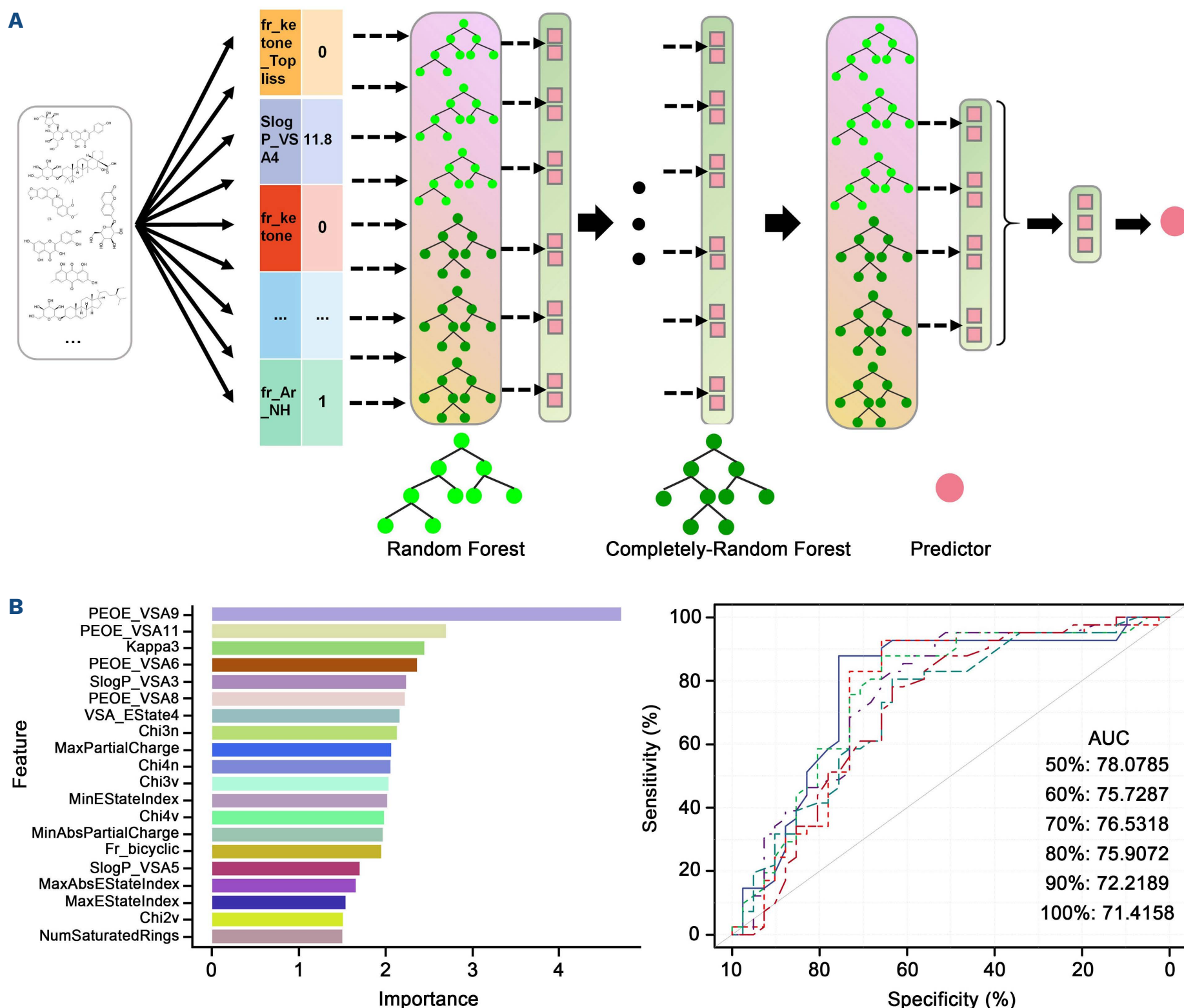
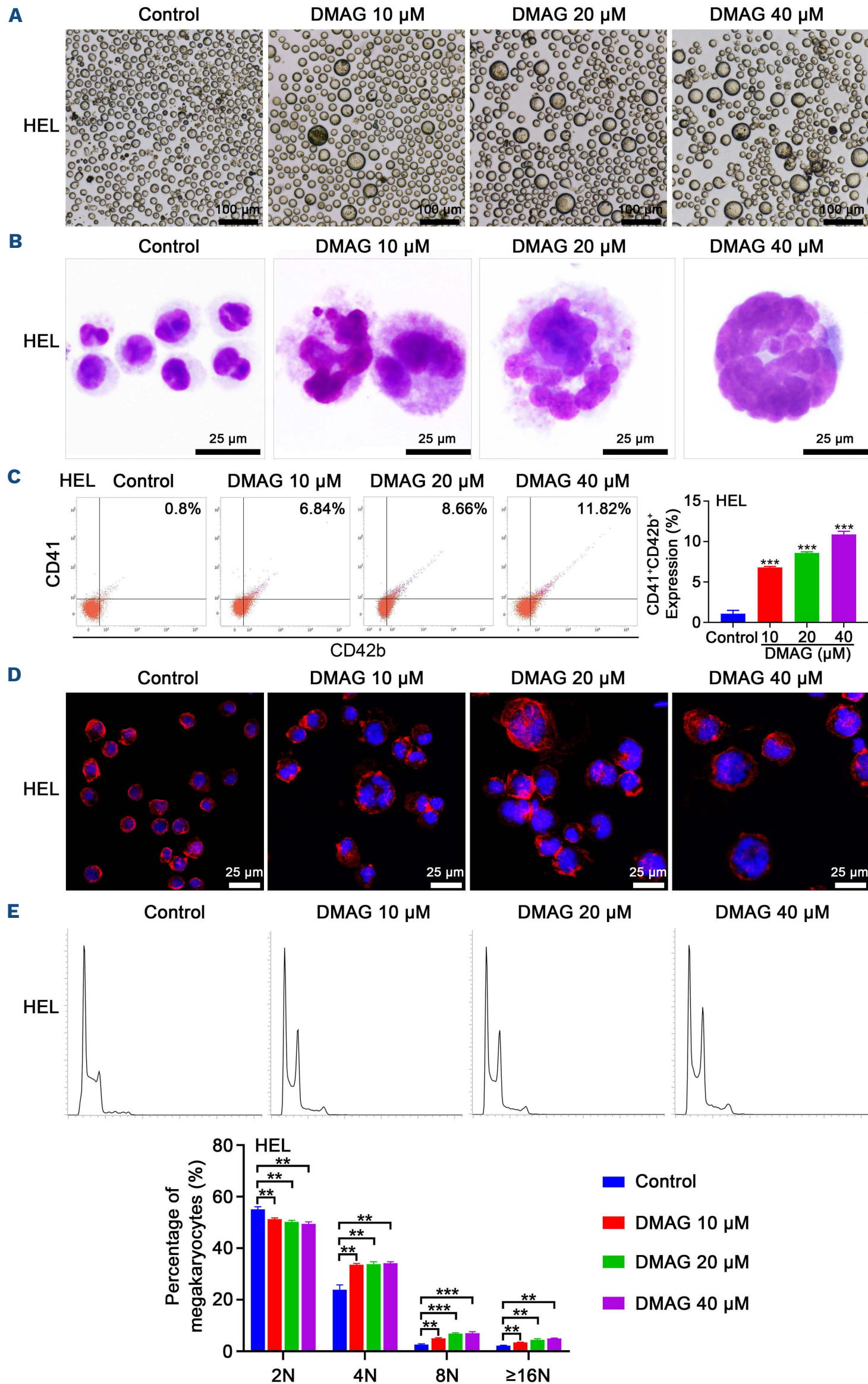


**Figure 1. Construction of the drug screening model.** (A) Flowchart for gcForest model construction. (B) Top 20 molecular descriptors. (C) Receiver operator characteristic curves of importance ratios. AUC: area under the curve.

analysis indicated that DMAG might promote megakaryocyte differentiation through the MAPK and HIF-1 signaling pathways. We therefore first determined the expression of MEK and ERK1/2, and HIF-1 $\alpha$  and HIF-1 $\beta$ , the key genes involved in the MAPK and HIF-1 signaling pathways, respectively. Our results showed that the phosphorylation of ERK1/2 and the expression of HIF-1 $\beta$  were continuously activated by DMAG from day 1 to day 6 (Figure 3C, *Online Supplementary Figure S3*). Other known cellular signaling pathways related to megakaryocyte differentiation were also investigated. DMAG treatment had no obvious effects on the activation of the c-MPL, JAK2/STAT and PI3K/AKT signaling pathways (Figure 3C, *Online Supplementary Figure S3*). These results suggest that DMAG promotes megakaryocyte differentiation by activating ERK1/2 and HIF-1 $\beta$ .

### The effect of DMAG on the expression of transcription factors participating in megakaryocyte differentiation

Several transcription factors drive megakaryocyte differentiation and platelet formation.<sup>3</sup> We thus examined the temporal expression pattern of NF-E2, GATA1, GATA2, FLI1, TAL1 and RUNX1 during DMAG-induced differentiation of HEL cells by quantitative real-time PCR. The results showed that the transcriptional level of *NFE2* in the DMAG-treated group was significantly higher than that in the control group from day 1 to day 6 (Figure 4A). The expression level of *GATA1* in the DMAG-treated group was higher than that in the control group from day 2 to day 5 (Figure 4A). In contrast, *RUNX1* expression in the DMAG-treated group was lower than that in the control group on days 1, 2, 3 and 5 (Figure 4A). *GATA2* expression in the DMAG-treated



Continued on following page.

**Figure 2. DMAG promotes megakaryocyte differentiation and enhances the DNA ploidy of HEL cells.** (A) Representative images of HEL cells treated with different concentrations of DMAG (10, 20 and 40  $\mu$ M) for 6 days. Bars represent 100  $\mu$ m. (B) Giemsa-Wright staining of HEL cells treated with different concentrations of DMAG (10, 20 and 40  $\mu$ M) for 6 days. Bars represent 25  $\mu$ m. (C) Flow cytometry analysis of the expression of CD41 and CD42b after cells had been treated with different concentrations of DMAG (10, 20 and 40  $\mu$ M) for 6 days. The histogram shows the percentage of CD41<sup>+</sup>CD42b<sup>+</sup> cells for each group. (D) Phalloidin staining of HEL cells treated with different concentrations of DMAG (10, 20 and 40  $\mu$ M) for 6 days. DAPI staining (blue) indicates nuclei, and TRITC phalloidin staining (red) of F-actin indicates the boundary of single cells. Bars represent 25  $\mu$ m. (E) Flow cytometry analysis of the DNA ploidy of HEL cells treated with different concentrations of DMAG (10, 20 and 40  $\mu$ M) for 6 days. The histogram shows the percentages of DNA ploidy of the HEL cells treated with the different concentrations of DMAG. In (C) and (E), data are shown as the mean  $\pm$  standard deviation from three independent experiments. \*\* $P < 0.01$ , \*\*\* $P < 0.001$ , versus the corresponding control. DMAG: 3,8-di-O-methylsuccinic acid 2-O-glucoside; DAPI: 4',6-diamidino-2-phenylindole.

group was higher than that in the control group at day 3 and decreased at days 4 and 5 (Figure 4A). *FLI1* expression in the DMAG-treated group was higher than that in the control group on day 4, becoming lower on day 5 and then higher again on day 6 (Figure 4A). There was no significant difference in *TAL1* expression level between the DMAG-treated group and the control group from day 1 to day 5 (Figure 4A). The translational levels of these transcription factors were also determined. Consistent with the transcriptional level, the translational level of NF-E2 in the DMAG-treated group was significantly higher than that in the control group from day 1 to day 6 (Figure 4B, *Online Supplementary Figure S4*). In contrast, the translational level of RUNX1 in the DMAG-treated group was lower than that in the control group on day 6 (Figure 4B, *Online Supplementary Figure S4*). However, DMAG had no conspicuous effect on the translational levels of GATA1, *TAL1* and *FOG1* (Figure 4B, *Online Supplementary Figure S4*). We further confirmed that DMAG treatment led to a dose-dependent increase in the expression of NF-E2 at the translational level (Figure 4B, *Online Supplementary Figure S4*). Moreover, the increased expression of NF-E2 induced by DMAG in HEL and Meg-01 cells was confirmed by immunofluorescence analysis (*Online Supplementary Figure S5A*).

The microtubule cytoskeleton plays a crucial role in the proper maturation of megakaryocytes and proplatelet formation.<sup>21</sup> We therefore determined the expression of  $\beta$ -tubulin, a protein subunit of microtubules, and found that HEL and Meg-01 cells treated with different concentrations of DMAG showed remarkable increases in  $\beta$ -tubulin expression (*Online Supplementary Figure S5B*). Collectively, these data suggest that DMAG promotes megakaryocyte differentiation through activation of NF-E2 and is probably able to promote proplatelet formation by increasing  $\beta$ -tubulin expression.

#### DMAG promotes megakaryocyte differentiation in an ERK1/2-HIF-1 $\beta$ -NF-E2-dependent pathway

Emerging evidence indicates that ERK is required for the transactivation activity of HIF-1 and that HIF-1 promotes the expression of NF-E2, which is closely related to hematopoietic regulation.<sup>22-25</sup> To clarify how they mediated

megakaryocyte differentiation induced by DMAG, a step-by-step blocking strategy was performed. First, the ERK1/2-specific inhibitor SCH772984 was used to block the phosphorylation of ERK1/2. When the phosphorylation of ERK1/2 induced by DMAG was blocked, the expression of HIF-1 $\beta$  and NF-E2 was significantly inhibited (Figure 5A, *Online Supplementary Figure S6*), which indicated that phosphorylation of ERK1/2 induced by DMAG was responsible for the activation of HIF-1 $\beta$  and NF-E2. Wright-Giemsa staining, DAPI and phalloidin staining and flow cytometry analysis further demonstrated that SCH772984 (10  $\mu$ M) treatment interrupted the acceleration of megakaryocyte differentiation induced by DMAG (Figure 5B-D). We also found that megakaryocyte differentiation induced by DMAG was significantly inhibited when NF-E2 was knocked down by siRNA interference (*Online Supplementary Figures S7 and S8*). These data demonstrate that DMAG promotes megakaryocyte differentiation in an ERK1/2-HIF-1 $\beta$ -NF-E2-dependent pathway.

#### DMAG enhances platelet recovery in mice with thrombocytopenia and accelerates thrombopoiesis in zebrafish

To investigate the potential therapeutic effect of DMAG in mice with thrombocytopenia induced by 4 Gy X-ray total body irradiation, KM mice were administered DMAG (5 mg/kg) for 17 days after radiation (Figure 6A). As shown, peripheral platelet levels in all irradiated groups dropped to the nadir on day 7 (Figure 6B). However, the numbers of peripheral platelets on day 7 were higher in the groups administered TPO or DMAG than in the irradiated group (Figure 6B). DMAG administration significantly increased the recovery of peripheral platelets in the irradiated mice from day 7 to day 14 (Figure 6B). The platelet counts of the DMAG-treated group recovered to almost 72% and 96% those of the control group at day 10 and day 14, respectively (Figure 6B), while the platelet counts in the irradiated group were only approximately 50% and 75% of those in the control group at day 10 and day 14, respectively (Figure 6B). There was no difference in the mean platelet volume between each group (*Online Supplementary Figure S9A*), which demonstrated that DMAG had no influence on mean platelet volume. There were no differences in the levels of

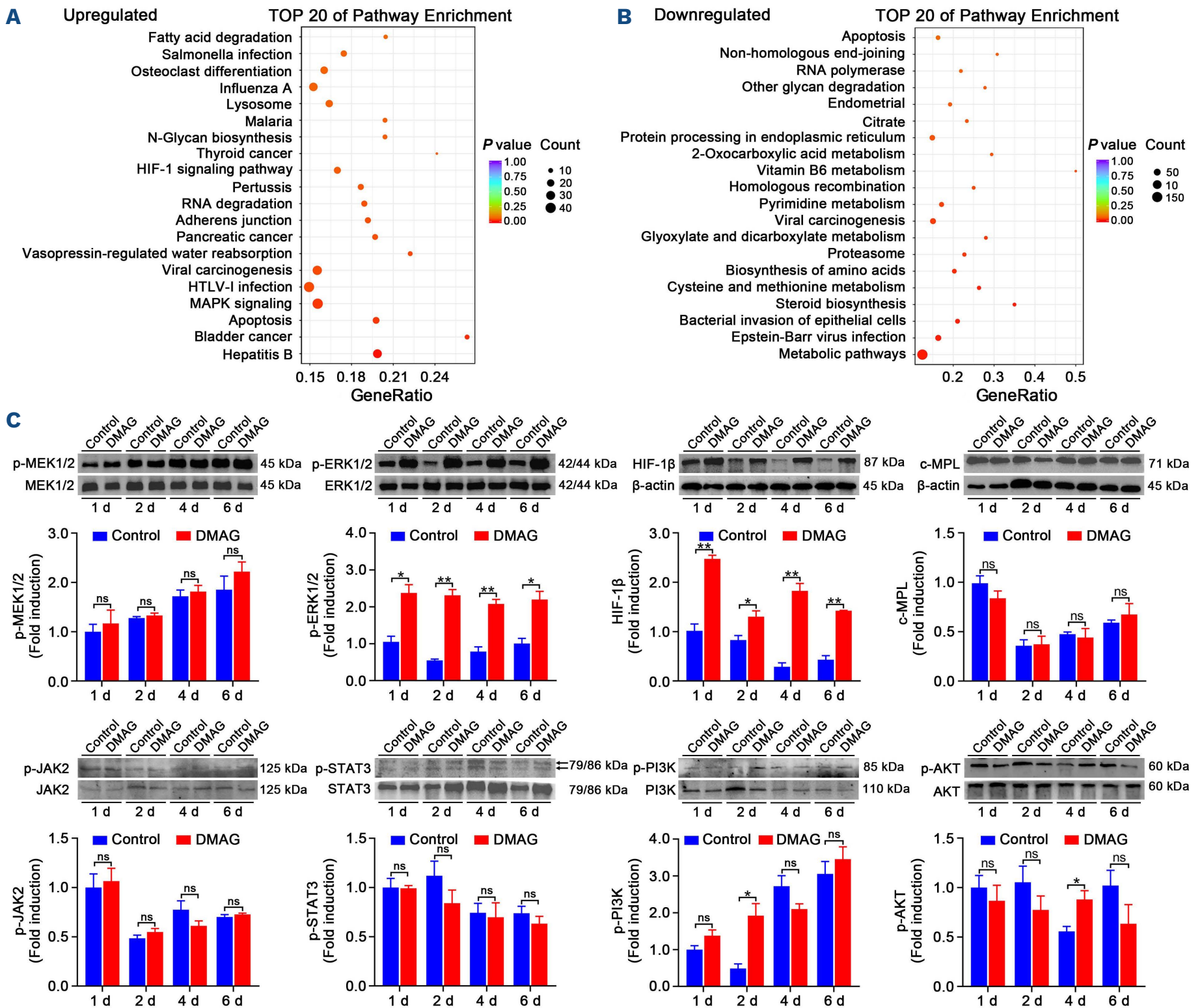


**Figure 3. DMAG activates the expression of ERK1/2 and HIF-1 $\beta$ .** (A, B) Top 20 enriched KEGG pathways targeted by upregulated mRNA (A) and downregulated mRNA (B) induced by DMAG. (C) Western blot analysis of proteins related to megakaryocyte differentiation after the cells were or were not treated with DMAG (40  $\mu$ M) at the indicated times. All results are shown as the mean  $\pm$  standard deviation of three independent experiments. \* $P < 0.05$ , \*\* $P < 0.01$ , or indicated as not significant (ns) versus the corresponding control. DMAG: 3,8-di-O-methylellagic acid 2-O-glucoside; KEGG: Kyoto Encyclopedia of Genes and Genomes.

red or white blood cells between the TPO-treated, DMAG-treated and irradiated groups at any of the tested time-points (Figure 6B), indicating that DMAG had a specific effect on platelet recovery. To verify whether the effect of DMAG on platelet recovery was stable, DMAG administration was ceased on day 18 and the platelet level was monitored sequentially. The platelet count of the DMAG-treated group was maintained at a normal level from day 19 to 25 (Online Supplementary Figure S9B), indicating that the effect of DMAG on platelet recovery was stable and durable. DMAG administration clearly increased the BM nuclear cell count (Online Supplementary Figure S9C), indicating that

DMAG could ameliorate irradiation-induced damage to BM nuclear cells or enhance their proliferation. The visceral indices of the spleen and thymus were examined and it was found that the thymus index was higher in the DMAG-treated group than in the irradiated group (Online Supplementary Figure S10), indicating that DMAG might be able to enhance immune function by alleviating thymus atrophy induced by irradiation.

To investigate whether the increase in peripheral platelets induced by DMAG was due to facilitation of megakaryopoiesis, hematoxylin and eosin (H&E) staining was performed and revealed that the numbers of megakaryocytes

in the BM and spleen were clearly increased after administration of DMAG for 10 days (Figure 6C-E). These data suggest that DMAG stimulation is conducive to *in vivo* platelet recovery after radiation.

To determine whether the platelets stimulated by DMAG

administration were functional, we measured platelet function. A carotid artery thrombosis model was used to assess the effect of DMAG on thrombus formation after vascular injury. The results showed that the time required to form a thrombus that completely occluded the artery

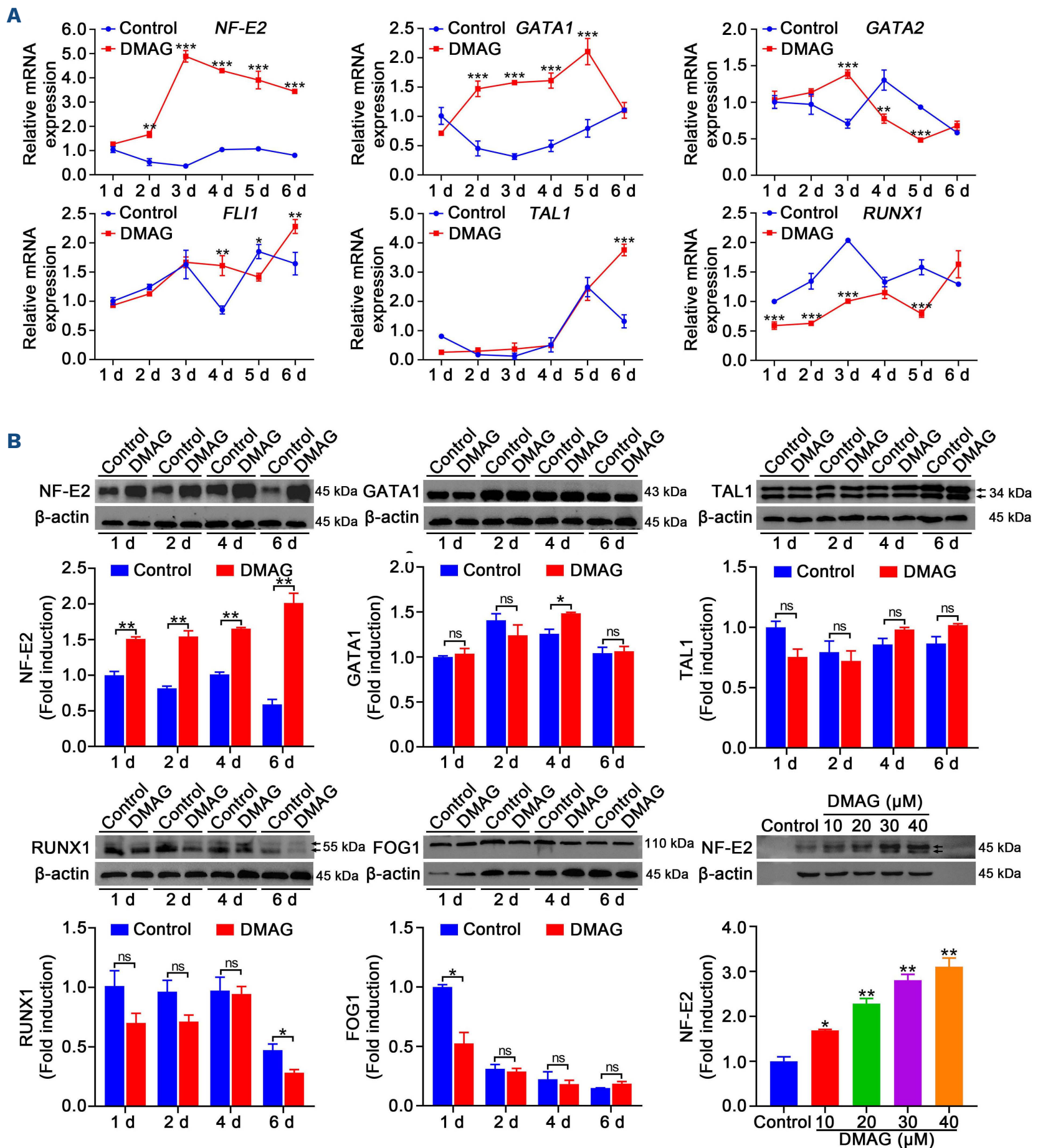


**Figure 4. Effects of DMAG on the expression of transcription factors related to megakaryocyte differentiation.** (A) Quantitative real-time polymerase chain reaction analysis of the expression of transcription factors involved in megakaryocyte differentiation after cells were or were not treated with DMAG (40 μM) for the indicated times. (B) Western blot detection of transcription factors related to megakaryocyte differentiation after the cells were or were not treated with DMAG (40 μM) for the indicated times or with different concentrations of DMAG (10, 20, 30 and 40 μM) for 3 days. Throughout, data are shown as the means ± standard deviations of three independent experiments. \* $P < 0.05$ , \*\* $P < 0.01$ , \*\*\* $P < 0.001$ , or indicated as not significant (ns) versus the corresponding control. DMAG: 3,8-di-O-methylellagic acid 2-O-glucoside.

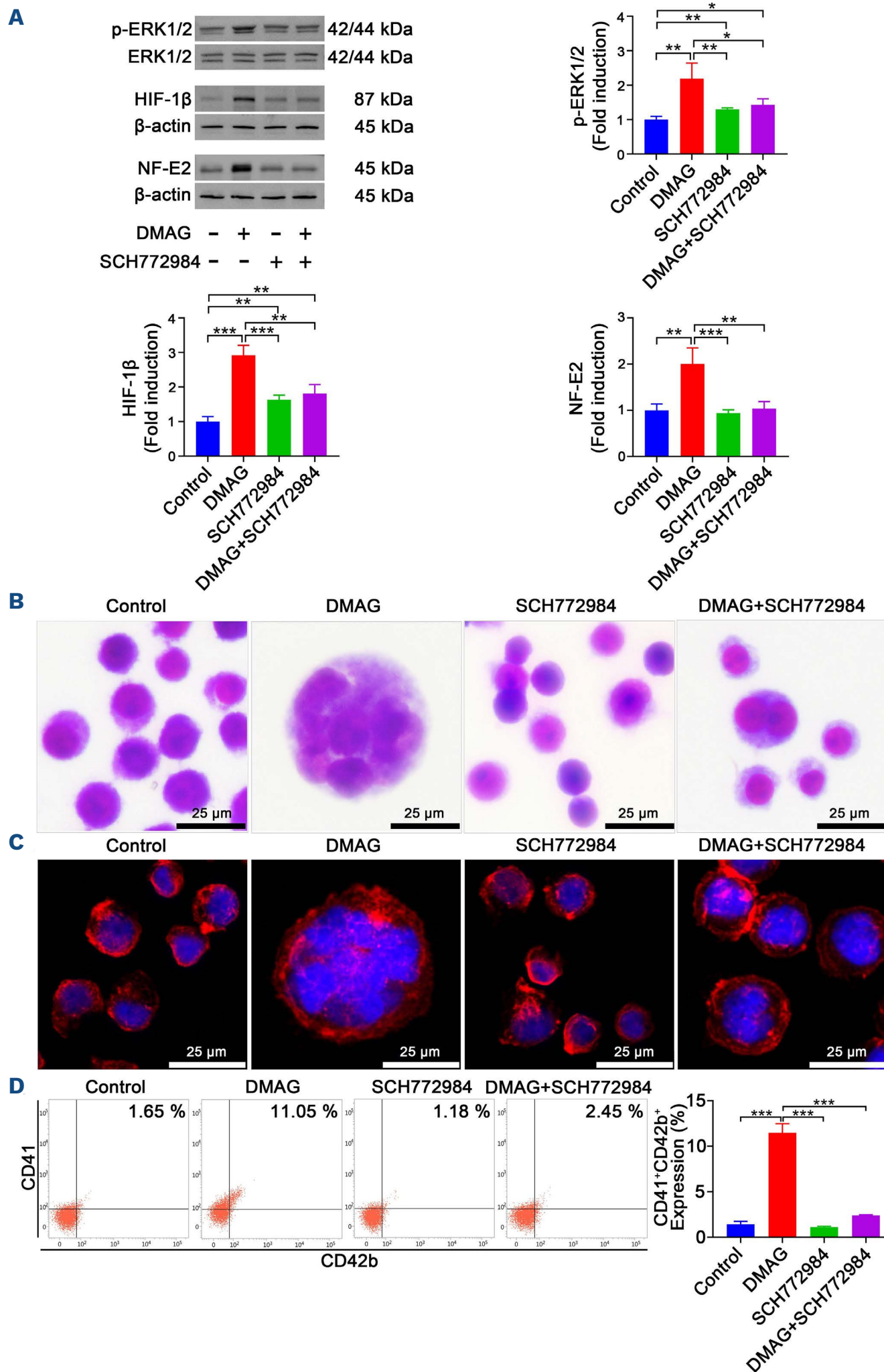


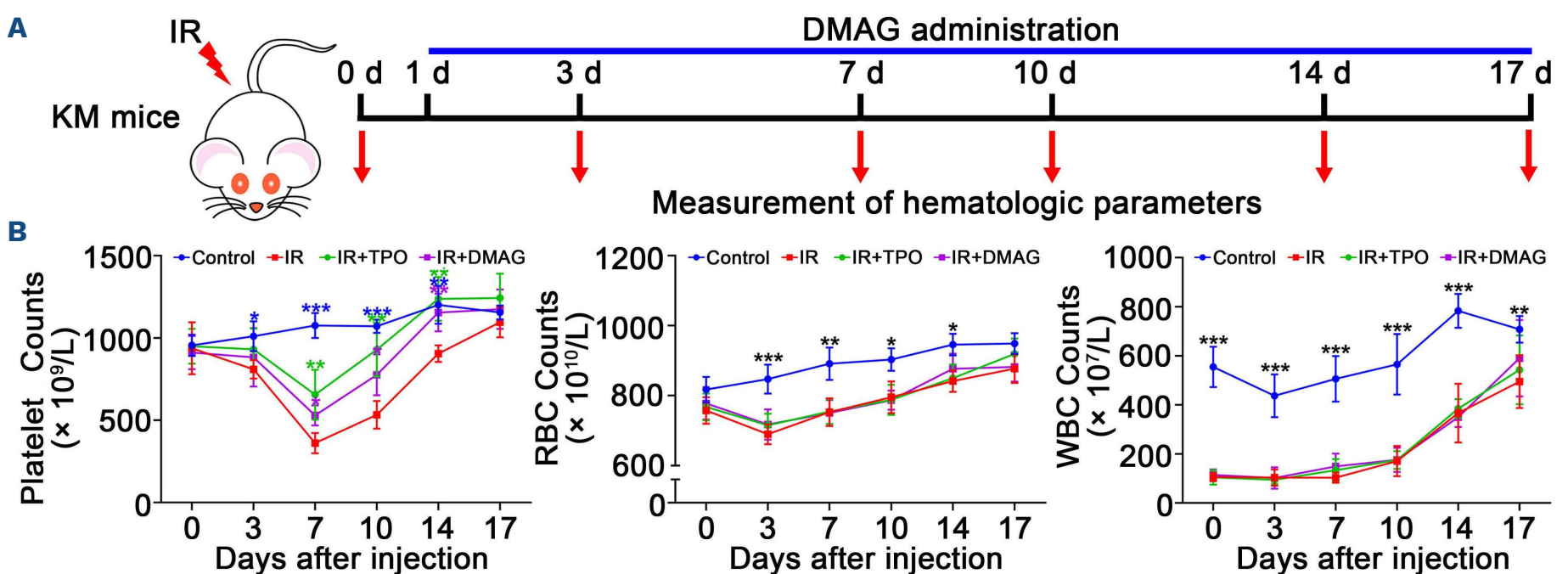
**Figure 5. The ERK1/2-HIF-1β-NF-E2 signaling pathway is involved in DMAG-induced megakaryocyte differentiation.** (A) Western blot analysis of ERK1/2 phosphorylation after HEL cells were pretreated with the ERK1/2 inhibitor SCH772984 (10 μM) followed by DMAG (40 μM) stimulation for 3 days. The histograms show the ratio of p-ERK/ERK, HIF-1β/β-actin and NF-E2/β-actin for each group. (B) Giemsa-Wright staining shows the effects of SCH772984 on DMAG (40 μM)-induced changes in cell morphology. Bars represent 25 μm. (C) Phalloidin staining shows the effects of SCH772984 on DMAG (40 μM)-induced multinuclear formation. Bars represent 25 μm. (D) Detection of the expression of CD41 and CD42b by flow cytometry indicates the effects of SCH772984 on DMAG (40 μM)-induced megakaryocyte differentiation. The histogram shows the percentage of CD41<sup>+</sup>CD42b<sup>+</sup> cells for each group. In (A) and (D), data are shown as the mean ± standard deviation from three independent experiments. \**P*<0.05, \*\**P*<0.01, \*\*\**P*<0.001, versus the corresponding control. DMAG: 3,8-di-O-methylsuccinic acid 2-O-glucoside.

after the initial arterial injury in the DMAG-treated group was significantly shorter than that in the irradiated group (*Online Supplementary Figure S11A*), suggesting that DMAG promoted thrombus formation in mice with thrombocytopenia. Moreover, collagen-induced platelet aggregation was measured and showed that platelet aggregation was enhanced by DMAG administration (*Online Supplementary Figure S11B*). These results demonstrate that DMAG can restore platelet function in mice with thrombocytopenia. To further evaluate the potential of DMAG for clinical translation, we investigated the *in vivo* toxicity of DMAG. Levels of markers of cardiac function markers (creatinine kinase, lactate acid dehydrogenase), hepatic function (alanine aminotransferase, aspartate aminotransferase) and renal function (creatinine, blood urea nitrogen) were determined after DMAG administration. There was no difference in creatine kinase content between each group (*Online Supplementary Figure S12A*), while the lactate dehydrogenase concentration in the DMAG-treated group was lower than that in the irradiated group (*Online Supplementary Figure S12A*), indicating that DMAG was beneficial to cardiac function. The levels of alanine and aspartate aminotransferases were not remarkable in any group (*Online Supplementary Figure S12A*), which suggested that DMAG had no effect on hepatic function. The creatinine and blood urea nitrogen levels in the control, TPO-treated and DMAG-treated groups were much lower than those in the irradiated group (*Online Supplementary Figure S12A*), indicating that DMAG was able to mitigate the renal toxicity induced by irradiation. In addition, H&E staining showed that there were no significant differences in the major organs between the groups (*Online Supplementary Figure S12B*), suggesting that DMAG did not cause any significant systemic toxicity. The above data suggest that DMAG has no toxicity *in vivo*; in contrast, DMAG exhibits protective effects on the heart

and kidney in thrombocytopenic mice. Taken together, these results demonstrate that DMAG has excellent therapeutic effects on mice with thrombocytopenia.

The enhanced numbers of megakaryocytes in the DMAG-treated group prompted us to investigate whether DMAG was able to promote the differentiation of hematopoietic progenitors into megakaryocytic progenitors and megakaryocytes in BM. Flow cytometry analysis showed that the proportions of c-Kit<sup>+</sup>CD41<sup>-</sup> (hematopoietic progenitors), c-Kit<sup>+</sup>CD41<sup>+</sup> (megakaryocytic progenitors), and c-Kit<sup>-</sup>CD41<sup>+</sup> (megakaryocytes) cells were significantly increased in the TPO- and DMAG-treated groups compared with the proportions in the irradiated group (*Online Supplementary Figure S13A*). The results suggest that DMAG can trigger the production of megakaryocytes at different stages of megakaryopoiesis.

The expression of the megakaryocyte-specific markers CD41 and CD61 was determined by flow cytometry. The results showed that the proportions of CD41<sup>+</sup>CD61<sup>+</sup> cells in the BM and spleen were remarkably higher in the TPO- and DMAG-treated groups than in the irradiated group (*Online Supplementary Figure S13B*), which indicates that DMAG promoted BM and spleen megakaryocyte differentiation. Flow cytometry was further used to analyze the DNA contents of BM megakaryocytes. As expected, the ploidy of BM megakaryocytes was significantly increased in the TPO- and DMAG-treated groups compared with the irradiated group (*Online Supplementary Figure S13C*). The expression of the platelet activation marker CD62P (platelet surface P-selectin) was detected by flow cytometry. We found that BM cells of the TPO- and DMAG-treated groups contained significantly higher percentages of platelets (CD41<sup>+</sup>CD62P<sup>+</sup>) than those in the irradiated group (*Online Supplementary Figure S13D*). However, activated platelets (CD41<sup>-</sup>CD62P<sup>+</sup>) were almost undetectable in all groups



Continued on following page.

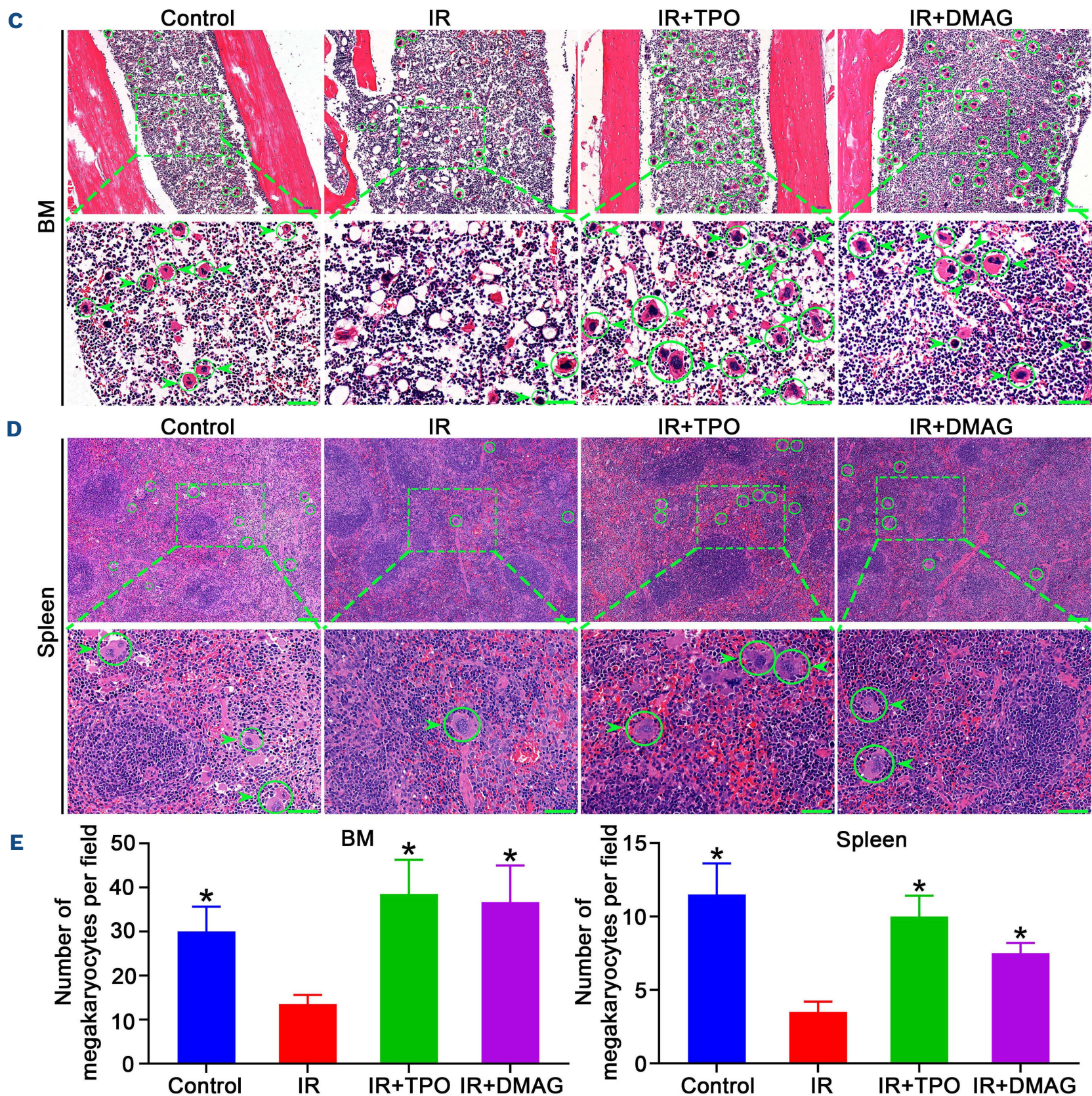


**Figure 6. DMAG administration counteracts radiation-induced thrombocytopenia *in vivo*.** (A) Schematic diagram of DMAG administration in KM mice with thrombocytopenia induced by irradiation. (B) Numbers of peripheral platelets, red blood cells and white blood cells in KM mice at the indicated times after injection of normal saline, thrombopoietin (3,000 U/kg), or DMAG (5 mg/kg) daily after irradiation. (C, D) Staining with hematoxylin and eosin shows the megakaryocytes in bone marrow (C) and spleen (D) after mice were treated with normal saline, thrombopoietin (3,000 U/kg) or DMAG (5 mg/kg) for 10 days. Ten microscopy fields per sample were counted. The green circles mark the megakaryocytes. (E) The histogram shows the number of megakaryocytes in the bone marrow and spleen in each group. In (B) and (E), the data are shown as the mean  $\pm$  standard deviation from three independent experiments. \* $P < 0.05$ , \*\* $P < 0.01$ , \*\*\* $P < 0.001$ , versus the irradiated group or corresponding control. KM: Kunming; IR: irradiation; DMAG: 3,8-di-O-methylellagic acid 2-O-glucoside; TPO: thrombopoietin; RBC: red blood cell; WBC: white blood cell; BM: bone marrow.

(Online Supplementary Figure S13D). These results indicate that DMAG accelerates thrombopoiesis in BM.

Although DMAG did not exert a stimulatory effect on red blood cell recovery in peripheral blood, we still examined the expression of the erythrocyte surface marker Ter119 in

BM cells. Unexpectedly, we found that the percentage of Ter119<sup>+</sup> cells was higher in the DMAG-treated group than in the irradiated group (Online Supplementary Figure S14), indicating that DMAG was able to promote erythropoiesis in BM. Furthermore, immunohistochemical staining was

carried out to detect the expression of CD41 and NF-E2. The results showed that the numbers of CD41<sup>+</sup> megakaryocytes in the TPO- and DMAG-treated groups were higher than the number in the irradiated group (*Online Supplementary Figure S15A*). Consistent with the findings of the *in vitro* experiments, NF-E2 expression in BM megakaryocytes in the DMAG-treated groups was significantly higher than that in the irradiated group (*Online Supplementary Figure S15A*). Serum TPO concentrations were measured and showed that there was no significant difference in TPO levels between the irradiated group and the DMAG-treated group (*Online Supplementary Figure S15B*), suggesting that DMAG does not influence TPO production. All these data indicate that DMAG rescues megakaryopoiesis, thereby accelerating the production of platelets in irradiated mice. The effects of DMAG on thrombopoiesis were further verified in zebrafish. Tg (cd41:eGFP) transgenic zebrafish were treated with DMAG (10, 25 and 50  $\mu$ M) at 3 days post-fertilization (dpf). As expected, the overall numbers of cd41:eGFP thrombocytes at 5 dpf were significantly higher in all the DMAG-treated groups than in the control group (Figure 7A). The dorsal aorta, caudal hematopoietic tissue and tail regions were then carefully observed for cd41:eGFP thrombocytes. It was seen that the numbers of cd41:eGFP cells in all three regions of the DMAG (10, 25 and 50  $\mu$ M)-treated groups were remarkably higher than those of the control group (Figure 7B-D). These results demonstrate that DMAG significantly promotes thrombopoiesis in zebrafish.

#### The effects of DMAG on megakaryopoiesis and thrombopoiesis are independent of TPO/c-MPL signaling

To gain a deeper understanding of whether DMAG-induced megakaryopoiesis and thrombopoiesis depend on TPO/c-MPL signaling *in vivo*, we used CRISPR/Cas9 technology to construct c-MPL<sup>-/-</sup> mice. We designed two sgRNA that could generate a 16 kb chromosomal deletion at the c-MPL locus in the mouse genome (Figure 8A, *Online Supplementary Figure S16*). After obtaining the c-MPL<sup>-/-</sup> mice, their peripheral platelet levels were measured, and they were found to have severely decreased numbers of platelets (Figure 8B). However, DMAG treatment significantly increased the peripheral platelet level in c-MPL<sup>-/-</sup> mice on days 7 and 10 (Figure 8B). There were no differences in red or white blood cell counts between the groups (Figure 8B). H&E staining showed that DMAG-treated c-MPL<sup>-/-</sup> mice had more megakaryocytes in the BM and spleen than control c-MPL<sup>-/-</sup> mice (Figure 8C, D). Corresponding to the H&E staining results, flow cytometry analysis showed that CD41<sup>+</sup> cells (megakaryocytes) were much more abundant in the BM and spleen of DMAG-treated c-MPL<sup>-/-</sup> mice than in control c-MPL<sup>-/-</sup> mice (*Online Supplementary Figure S17A*). Accordingly, the population of megakaryocytic progenitors (c-Kit<sup>+</sup>CD41<sup>+</sup>) was significantly increased in DMAG-

treated c-MPL<sup>-/-</sup> mice compared to that in control c-MPL<sup>-/-</sup> mice (*Online Supplementary Figure S17B*). Finally, the platelet surface marker CD41<sup>+</sup>CD62P<sup>+</sup> was measured by flow cytometry. The results showed that the number of platelets (CD41<sup>+</sup>CD62P<sup>+</sup>) in the BM of c-MPL<sup>-/-</sup> mice was increased after DMAG administration (*Online Supplementary Figure S17C*). Collectively, the above results indicate that DMAG is capable of functioning in a TPO-independent manner in promoting megakaryopoiesis and thrombopoiesis *in vivo*.

We also investigated whether DMAG had a stimulatory effect on thrombopoiesis in normal mice. Normal C57BL/6 mice were administered DMAG for 14 consecutive days, and hematologic parameters were measured. Interestingly, we found that DMAG treatment had no effects on peripheral platelet, red blood cell or white blood cell levels (*Online Supplementary Figure S18A*). Furthermore, H&E staining data demonstrated that the numbers of megakaryocytes in the BM and spleen were not different between the control and DMAG-treated groups (*Online Supplementary Figure S18B, C*). These data indicate that DMAG has a unique therapeutic effect on mice with thrombocytopenia.

## Discussion

Thrombocytopenia is common finding in a multitude of conditions,<sup>3,5-7</sup> and can sometimes be life-threatening because of bleeding complications, which in turn profoundly influence subsequent therapies for the diseases.<sup>26</sup> However, there are few medical treatments available for thrombocytopenia. The discovery and development of a new drug is an extremely long and costly process, and the success rate is piteously low.<sup>13</sup> It is, therefore, critical to develop new approaches that can substantially decrease costs and accelerate the drug discovery process. The adoption of machine learning approaches is ideally suited to do this. The application of machine learning in drug discovery not only decreases the costs, labor and time required to find the ideal compounds from months or years to weeks but also increases the true positive rate to identify structurally novel compounds with the desired bioactivity from thousands of chemical compounds.<sup>12</sup> In this study, we developed a drug screening model in hematopoiesis based on a novel gcForest algorithm and virtual screening of potential active compounds from a chemical library. Encouragingly, we found that a natural product, DMAG, not only significantly promoted megakaryocyte differentiation and maturation *in vitro* but also stimulated platelet recovery in thrombocytopenic mice and the c-MPL<sup>-/-</sup> mouse model, and promoted thrombopoiesis in zebrafish.

In a previous study we demonstrated that DMAG can be

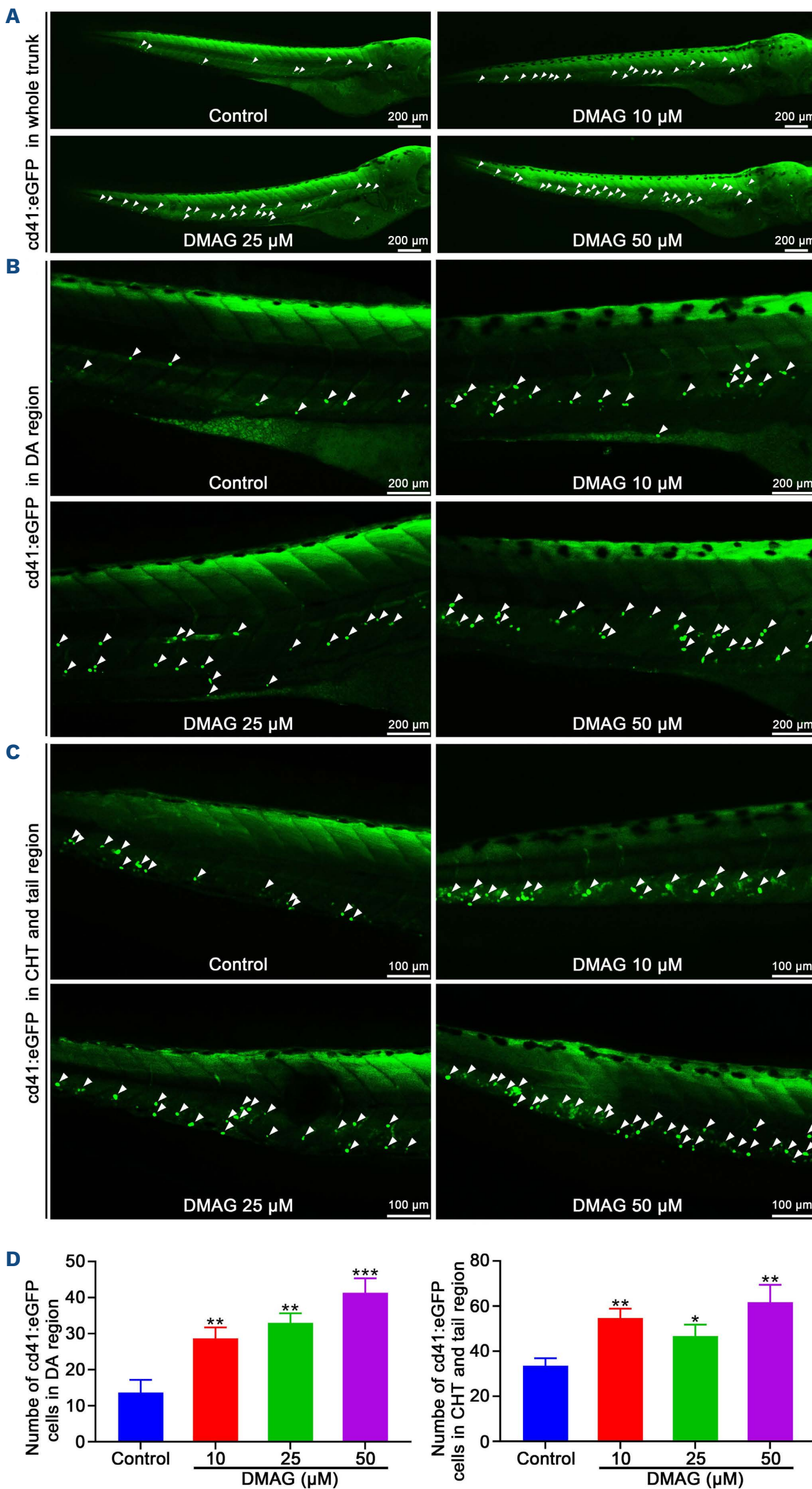
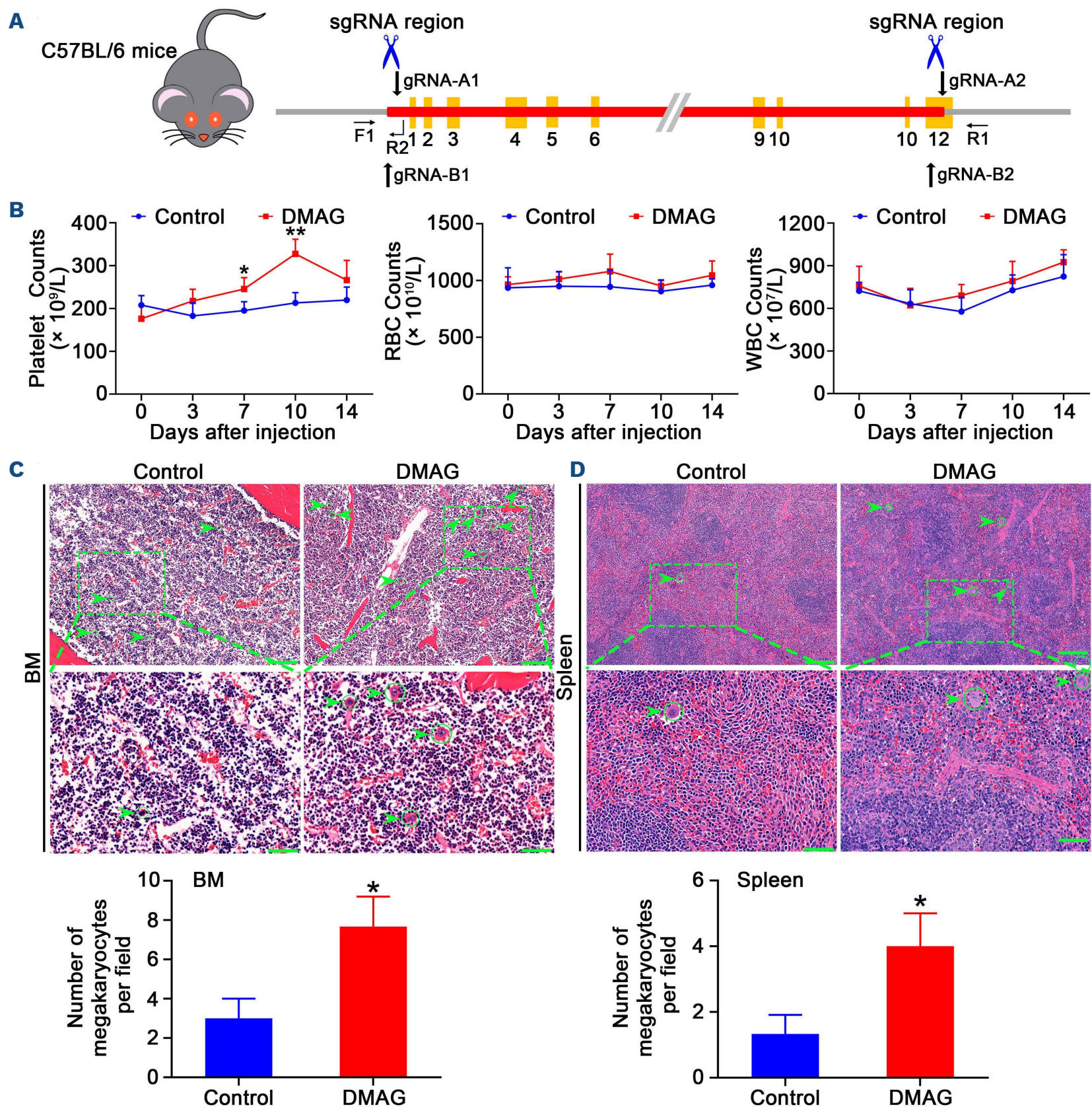


**Figure 7. DMAG administration enhances thrombopoiesis in Tg (cd41:eGFP) transgenic zebrafish.** (A-C) cd41:eGFP thrombocytes in whole trunk (A), dorsal aorta (B), caudal hematopoietic tissue and tail regions (C) of control and DMAG (10, 25 and 50 μM)-treated zebrafish. (D) Quantification of cd41:eGFP cells in the dorsal aorta, caudal hematopoietic tissue and tail regions in each group. The data are shown as the mean ± standard deviation from three independent experiments. \* $P < 0.05$ , \*\* $P < 0.01$ , \*\*\* $P < 0.001$ , versus the corresponding control. DMAG: 3,8-di-O-methylellagic acid 2-O-glucoside; DA: dorsal aorta; CHT: caudal hematopoietic tissue.

separated from a traditional Chinese medicine *Sanguisorba officinalis* L.<sup>27</sup> *Sanguisorba officinalis* L. is reported to possess hemostatic and anti-leukopenia activities,<sup>28</sup> and its active compounds are worthy of future study. Here, we demonstrated that DMAG continuously activated ERK1/2 and HIF-1 $\beta$  expression but did not activate TPO/c-MPL signaling or its other downstream signaling pathways. Our results are consistent with previous reports that ERK1/2 is a key regulator of differentiation of megakaryocytes and can act independently of TPO signaling.<sup>29-32</sup> HIF-1 $\alpha$  is a positive regulator of megakaryocyte maturation and platelet formation.<sup>21</sup> Previous studies have demonstrated that HIF-1 $\beta$  is crucial for hematopoiesis.<sup>33-35</sup> However, its

role in megakaryocyte differentiation and platelet formation is largely unknown. Here, we did not find any change in HIF-1 $\alpha$  expression between the control and DMAG-treated groups, whereas the expression of HIF-1 $\beta$  was continuously activated by DMAG. We assume that the continuous activation of HIF-1 $\beta$  is advantageous to the formation of fully active HIF-1, thereby enhancing the expression of genes related to megakaryocyte differentiation.

We determined the expression of transcription factors involved in megakaryocyte differentiation and platelet production and found that NF-E2 was continuously activated by DMAG in a concentration-dependent manner. Studies



Continued on following page.

**Figure 8. DMAG administration promotes megakaryopoiesis and thrombopoiesis in the c-MPL<sup>-/-</sup> mouse model.** (A) Schematic of the construction of the c-MPL<sup>-/-</sup> mouse model. The blue shears represent sgRNA regions (total size: 14.72 kb). The red line indicates the genomic region of the mouse c-MPL locus. The gray lines represent untranslated regions. The yellow rectangles mark 12 exons of c-MPL. F1, R1 and R2 show the primers used to identify the genotypes of the pups by polymerase chain reaction. (B) Numbers of peripheral platelets, red blood cells and white blood cells in c-MPL<sup>-/-</sup> mice at the indicated times after administration of normal saline or DMAG (5 mg/kg) daily for 14 consecutive days. (C, D) Hematoxylin and eosin staining shows the distribution of megakaryocytes in the bone marrow (C) and spleen (D) of the control and DMAG-treated groups injected with normal saline or DMAG (5 mg/kg) for 10 consecutive days. Bars represent 100  $\mu$ m (top) and 50  $\mu$ m (bottom). Ten microscopy fields per sample were counted. The green circles mark the megakaryocytes. The histogram shows the number of megakaryocytes in the bone marrow (C) and spleen (D) in each group. In (B-D), the data are shown as the mean  $\pm$  standard deviation from three independent experiments. \* $P$ <0.05, \*\* $P$ <0.01, versus the corresponding control. DMAG: 3,8-di-O-methylellagic acid 2-O-glucoside; RBC: red blood cell; WBC: white blood cells; BM: bone marrow.

have shown that NF-E2 is essential for megakaryocyte differentiation and maturation, proplatelet formation and platelet release, independently of the actions of TPO.<sup>36-39</sup> We also found that the expression of  $\beta$ -tubulin was significantly enhanced by DMAG in a dose-dependent manner. Tubulin is the major component of microtubules, consisting of  $\alpha$ -tubulin and  $\beta$ -tubulin.<sup>40</sup>  $\beta$ 1-tubulin (TUBB1) is the major  $\beta$ -tubulin isoform that is essential for megakaryocyte maturation and proplatelet formation.<sup>41-43</sup> It has been revealed that  $\beta$ 1-tubulin is one of the targets of NF-E2. The function of  $\beta$ 1-tubulin in platelet biogenesis is dependent on NF-E2.<sup>44</sup> In our study, the enhanced expression of  $\beta$ -tubulin induced by DMAG may have been mediated by NF-E2, which could be conducive to proplatelet formation. Through treatment with the ERK1/2-specific inhibitor SCH772984, we found that the upregulation of HIF-1 $\beta$  and NF-E2 induced by DMAG was blocked. The results indicated that ERK1/2 is located upstream of HIF-1 $\beta$  and NF-E2. These results are consistent with previous reports that ERK is able to regulate HIF-1 transactivation activity and stability and that HIF-1 $\alpha$  upregulates the expression of NF-E2 to promote hematopoiesis. In addition, the expression of NF-E2 is upregulated in polycythemic patients with augmented HIF signaling.<sup>25</sup> These findings indicate that NF-E2 may be a target of HIF-1. Therefore, an ERK1/2-HIF-1 $\beta$ -NF-E2-dependent pathway may mediate the effects of DMAG on megakaryocyte differentiation.

The therapeutic action of DMAG on thrombocytopenic mice highlights the importance of a strategy of inducing megakaryocyte differentiation for the treatment of thrombocytopenia, a strategy that could be considered a type of “autotransfusion” of platelets from already existing megakaryocytes in BM. In this study we found that platelet counts in irradiated mice decreased to the lowest level at day 7 after irradiation. The platelet counts in the groups of mice exposed to irradiation, TPO or DMAG were only 34%, 61% and 49%, respectively, of the platelet count of the control group, but the platelet count in the DMAG-treated group was 47% more than that in the irradiated group. The platelet counts recovered gradually from day 7 to day 14. The platelet counts in the DMAG-treated group recovered to almost 72% and 96% of those

in the control group at day 10 and 14, respectively. Nevertheless, the platelet counts in the irradiated group were only 50% and 75% of those in the control group at day 10 and 14, respectively. The platelet counts in the DMAG-treated group were almost 1.5- and 1.3-fold higher than those in the irradiated group at day 10 and 14, respectively. These data demonstrate that DMAG has an excellent ability to stimulate platelet recovery after radiation-induced damage. Moreover, DMAG was able to enhance megakaryopoiesis and thrombopoiesis in c-MPL<sup>-/-</sup> mice although it did not restore platelet counts to normal levels. The results indicate that DMAG promotes megakaryocyte differentiation and platelet formation in a TPO-independent manner, or at least in part in a TPO-independent manner. Previous studies have demonstrated that although knockout of TPO or c-MPL causes severe thrombocytopenia, the knockout mice are still able to produce a small but sufficient number of platelets to ensure their normal existence and show no symptoms of spontaneous hemorrhage.<sup>45</sup> TPO can stimulate megakaryocyte formation but cannot shorten the maturation time of these cells *in vivo*.<sup>46</sup> In addition, humans who have completely lost the function of c-MPL still have a certain number of platelets, indicating that patients without TPO/c-MPL signaling do possess some ability to produce platelets.<sup>10</sup> Recent studies have revealed that an inflammatory cytokine, chemokine ligand 5 (CCL5, RANTES), promotes megakaryocyte maturation and proplatelet formation in a CCR5-dependent manner and enhances platelet levels in response to physiological stress.<sup>47</sup> Taisuke *et al.*<sup>48</sup> showed that an activated form of tyrosyl-tRNA synthetase (YRS<sup>ACT</sup>) enhances megakaryopoiesis and platelet production in a TPO-independent manner. Rayko *et al.*<sup>49</sup> reported that iron deficiency increases megakaryocyte differentiation and platelet counts independently of TPO. Wang *et al.*<sup>30-32,50</sup> demonstrated that several hormones, including human growth hormone, norepinephrine, epinephrine, melatonin, as well as insulin-like growth factor-1, promote megakaryocyte differentiation, proplatelet formation, or platelet production in a TPO-independent manner. These findings and our study suggest that alternative mediators exist and seem able to compensate for the function of TPO when TPO/c-MPL signal-

ing is lost or that they and TPO may act synergistically in regulating megakaryocyte differentiation and platelet formation.

The influence of DMAG in normal mice was investigated. Interestingly, we found that DMAG had no effect on peripheral platelet count or megakaryocyte number in BM in normal mice, indicating that DMAG does not influence thrombopoiesis when the platelet count is normal. We hypothesize that the TPO/c-MPL signaling pathway may have a predominant function in regulating megakaryocyte differentiation and thrombopoiesis under normal conditions. When the TPO/c-MPL signaling pathway is disrupted, the function of the TPO-independent signaling pathway induced by DMAG may stand out. The unique therapeutic action of DMAG in pathological conditions may circumvent a risk of thrombosis.

Because DMAG promotes megakaryocyte differentiation and platelet formation in a TPO-independent manner, it has the potential for use to treat thrombocytopenia in patients who are unresponsive to TPO-receptor agonists or have a complete loss of functional c-MPL. Moreover, because of distinct mechanisms of action, the combined application of DMAG with TPO-receptor agonists may have a better therapeutic effect than a single drug in patients with thrombocytopenia. Collectively, the results of our study demonstrate that DMAG, derived from *Sanguisorba officinalis* L., stimulates megakaryocyte differentiation and platelet formation through the ERK1/2-HIF-1 $\beta$ -NF-E2 pathway, which is independent of the TPO signaling pathway (*Online Supplementary Figure S19*). Our findings provide new insights into alternative treatment options for treating thrombocytopenia.

In summary, our study is the first to establish a drug screening model in hematopoiesis using the gcForest algorithm and demonstrates that DMAG significantly promotes megakaryocyte differentiation and platelet formation. Mechanistically, the action of DMAG involves the TPO-independent ERK/HIF-1/NF-E2 signaling pathway. Our study shows the therapeutic utility of DMAG for thrombocytopenia and provides a new approach for high-throughput drug screening and the treatment of hematologic diseases by targeting TPO-independent signaling.

## Disclosures

No conflicts of interest to disclose.

## Contributions

JMW, AGW and CXZ conceived and designed the experiments and supervised all the research. JSL and QM developed the drug screening model. LW, SL, TZ and XXL performed the *in vitro* experiments. JY and JZ constructed the mouse model. JPC and WJZ analyzed the RNA-sequencing data. LW, SL, MR, FHH and AGW carried out the *in vivo* experiments. CXZ and WJZ provided the experimental platform. LW, JMW and JSL analyzed the data and wrote the original manuscript. JMW, QBM and CXZ revised the manuscript. All authors approved the final version of the manuscript.

## Funding

This work was supported by grants from the Natural Science Foundation of China (82204666, 82074129, 81903829 and 81804221, China), Sichuan Science and Technology Program (2022JDJQ0061, 2019YJ0484, 2019YFSY0014, 2019JDPT0010, and 2019YJ0473, China), the Special Research Project of Sichuan Province Administration of Traditional Chinese Medicine (2018JC013 and 2018JC038, China), the Research Project of Sichuan Provincial Education Department (18TD0051 and 18ZA0525, China), the Luzhou Science and Technology Project (2017-S-39(3/5), China), the Joint Project of Luzhou Municipal People's Government and Southwest Medical University (2018LZXNYD-ZK31, 2018LZXNYD-ZK49, 2019LZXNYD-J11, 2019LZXNYDJ05, 2018LZXNYD-ZK41, 2020LZXNYDZ03, 2020LZXNYDP01 and 2018LZXNYD-YL05, China), the School-level Fund of Southwest Medical University (2021ZKMS044, 2021ZKQN022, 2021ZKMS041, 2018-ZRZD-001, 2019-ZZD-006, 2017-ZRZD-017 and 2017-ZRQN-081, China), and the National innovation and entrepreneurship training program for college students, China (201910632002, 201910634003, China).

## Data-sharing statement

The authors will make their original data available to future researchers upon request directed to the corresponding author.

## References

1. Bianchi E, Norfo R, Pennucci V, et al. Genomic landscape of megakaryopoiesis and platelet function defects. *Blood*. 2016;127(10):1249-1259.
2. Leblanc R, Peyruchaud O. Metastasis: new functional implications of platelets and megakaryocytes. *Blood*. 2016;128(1):24-31.
3. Eto K, Kunishima S. Linkage between the mechanisms of thrombocytopenia and thrombopoiesis. *Blood*. 2016;127(10):1234-1241.
4. Li W, Morrone K, Kambhampati S, et al. Thrombocytopenia in MDS: epidemiology, mechanisms, clinical consequences and novel therapeutic strategies. *Leukemia*. 2016;30(3):536-544.
5. Tamamyian G, Danielyan S, Lambert M. Chemotherapy induced thrombocytopenia in pediatric oncology. *Crit Rev Oncol Hematol*. 2016;99:299-307.
6. Yamaguchi M, Hirouchi T, Yoshioka H, et al. Diverse functions of the thrombopoietin receptor agonist romiplostim rescue individuals exposed to lethal radiation. *Free Radic Biol Med*.

- 2019;136:60-75.
7. Izak M, Bussel JB. Management of thrombocytopenia. *F1000Prime Rep.* 2014;6:45.
  8. Ghanima W, Cooper N, Rodeghiero F, et al. Thrombopoietin receptor agonists: ten years later. *Haematologica.* 2019;104(6):1112-1123.
  9. Poston J, Gernsheimer T. Glucocorticoids promote response to thrombopoietin-receptor agonists in refractory ITP: a case series. *Int J Hematol.* 2019;110(2):255-259.
  10. van den Oudenrijn S, Bruin M, Folman CC, et al. Mutations in the thrombopoietin receptor, Mpl, in children with congenital amegakaryocytic thrombocytopenia. *Br J Haematol.* 2000;110(2):441-448.
  11. Ballmaier M, Germeshausen M. Congenital amegakaryocytic thrombocytopenia: clinical presentation, diagnosis, and treatment. *Semin Thromb Hemost.* 2011;37(6):673-681.
  12. Gupta R, Srivastava D, Sahu M, et al. Artificial intelligence to deep learning: machine intelligence approach for drug discovery. *Mol Divers.* 2021;25(3):1315-1360.
  13. Stokes JM, Yang K, Swanson K, et al. A deep learning approach to antibiotic discovery. *Cell.* 2020;180(4):688-702.
  14. Zhu J, Wang J, Wang X, et al. Prediction of drug efficacy from transcriptional profiles with deep learning. *Nat Biotechnol.* 2021;39(11):1444-1452.
  15. Dong Y, Yang W, Wang J, et al. MLW-gcForest: a multi-weighted gcForest model towards the staging of lung adenocarcinoma based on multi-modal genetic data. *BMC Bioinformatics.* 2019;20(1):578.
  16. Li Y, Zhang Q, Liu Z, et al. Deep forest ensemble learning for classification of alignments of non-coding RNA sequences based on multi-view structure representations. *Brief Bioinform.* 2021;22(4):bbaa354.
  17. Li Y, Li R, Feng Z, et al. Linagliptin regulates the mitochondrial respiratory reserve to alter platelet activation and arterial thrombosis. *Front Pharmacol.* 2020;11:585612.
  18. Wang L, Zhang T, Liu S, et al. Discovery of a novel megakaryopoiesis enhancer, ingenol, promoting thrombopoiesis through PI3K-Akt signaling independent of thrombopoietin. *Pharmacol Res.* 2022;177:106096.
  19. Cong L, Ran FA, Cox D, et al. Multiplex genome engineering using CRISPR/Cas systems. *Science.* 2013;339(6121):819-823.
  20. Qi J, You T, Pan T, et al. Downregulation of hypoxia-inducible factor-1 $\alpha$  contributes to impaired megakaryopoiesis in immune thrombocytopenia. *Thromb Haemost.* 2017;117(10):1875-1886.
  21. Poulter N, Thomas S. Cytoskeletal regulation of platelet formation: coordination of F-actin and microtubules. *Int J Biochem Cell Biol.* 2015;66:69-74.
  22. Li Z, Zhou W, Zhang Y, Sun W, et al. ERK regulates HIF1 $\alpha$ -mediated platinum resistance by directly targeting PHD2 in ovarian cancer. *Clin Cancer Res.* 2019;25(19):5947-5960.
  23. Minet E, Arnould T, Michel G, et al. ERK activation upon hypoxia: involvement in HIF-1 activation. *FEBS Lett.* 2000;468(1):53-58.
  24. Xie Y, Li W, Feng J, et al. MicroRNA-363 and GATA-1 are regulated by HIF-1 $\alpha$  in K562 cells under hypoxia. *Mol Med Rep.* 2016;14(3):2503-2510.
  25. Kapralova K, Lanikova L, Lorenzo F, et al. RUNX1 and NF-E2 upregulation is not specific for MPNs, but is seen in polycythemic disorders with augmented HIF signaling. *Blood.* 2014;123(3):391-394.
  26. Roweth H, Parvin S, Machlus K. Megakaryocyte modification of platelets in thrombocytopenia. *Curr Opin Hematol.* 2018;25(5):410-415.
  27. Long W, Liu S, Li XX, et al. Whole transcriptome sequencing and integrated network analysis elucidates the effects of 3,8-di-O-methylellagic acid 2-O-glucoside derived from *Sanguisorba officinalis* L., a novel differentiation inducer on erythroleukemia cells. *Pharmacol Res.* 2021;166:105491.
  28. Wang L, Li H, Shen X, et al. Elucidation of the molecular mechanism of *Sanguisorba officinalis* L. against leukopenia based on network pharmacology. *Biomed Pharmacother.* 2020;132:110934.
  29. Mazharian A, Watson S, Séverin S. Critical role for ERK1/2 in bone marrow and fetal liver-derived primary megakaryocyte differentiation, motility, and proplatelet formation. *Exp Hematol.* 2009;37(10):1238-1249.
  30. Chen S, Du C, Shen M, et al. Sympathetic stimulation facilitates thrombopoiesis by promoting megakaryocyte adhesion, migration, and proplatelet formation. *Blood.* 2016;127(8):1024-1035.
  31. Xu Y, Wang S, Shen M, et al. hGH promotes megakaryocyte differentiation and exerts a complementary effect with c-Mpl ligands on thrombopoiesis. *Blood.* 2014;123(14):2250-2260.
  32. Chen S, Qi Y, Wang S, et al. Melatonin enhances thrombopoiesis through ERK1/2 and Akt activation orchestrated by dual adaptor for phosphotyrosine and 3-phosphoinositides. *J Pineal Res.* 2020;68(3):e12637.
  33. Adelman D, Maltepe E, Simon M. Multilineage embryonic hematopoiesis requires hypoxic ARNT activity. *Genes Dev.* 1999;13(19):2478-2483.
  34. Ramírez-Bergeron D, Runge A, Adelman D, et al. HIF-dependent hematopoietic factors regulate the development of the embryonic vasculature. *Dev Cell.* 2006;11(1):81-92.
  35. Krock BL, Eisinger-Mathason TS, Giannoukos DN, et al. The aryl hydrocarbon receptor nuclear translocator is an essential regulator of murine hematopoietic stem cell viability. *Blood.* 2015;125(21):3263-3272.
  36. Shivdasani RA, Rosenblatt MF, Zucker-Franklin D, et al. Transcription factor NF-E2 is required for platelet formation independent of the actions of thrombopoietin/MGDF in megakaryocyte development. *Cell.* 1995;81(5):695-704.
  37. Shivdasani RA. The role of transcription factor NF-E2 in megakaryocyte maturation and platelet production. *Stem Cells.* 1996;14Suppl1:112-115.
  38. Fock E, Yan F, Pan S, et al. NF-E2-mediated enhancement of megakaryocytic differentiation and platelet production in vitro and in vivo. *Exp Hematol.* 2008;36(1):78-92.
  39. Fujita R, Takayama-Tsujimoto M, Satoh H, et al. NF-E2 p45 is important for establishing normal function of platelets. *Mol Cell Biol.* 2013;33(14):2659-2670.
  40. McKean P, Vaughan S, Gull K. The extended tubulin superfamily. *J Cell Sci.* 2001;114(Pt 15):2723-2733.
  41. Wang D, Villasante A, Lewis S, et al. The mammalian beta-tubulin repertoire: hematopoietic expression of a novel, heterologous beta-tubulin isotype. *J Cell Biol.* 1986;103(5):1903-1910.
  42. Schwer H, Lecine P, Tiwari S, et al. A lineage-restricted and divergent beta-tubulin isoform is essential for the biogenesis, structure and function of blood platelets. *Curr Biol.* 2001;11(8):579-586.
  43. Seo H, Chen SJ, Hashimoto K, et al. A  $\beta$ 1-tubulin-based megakaryocyte maturation reporter system identifies novel drugs that promote platelet production. *Blood Adv.* 2018;2(17):2262-2272.
  44. Lecine P, Italiano J, Kim S, et al. Hematopoietic-specific beta 1 tubulin participates in a pathway of platelet biogenesis dependent on the transcription factor NF-E2. *Blood.* 2000;96(4):1366-1373.
  45. Kimura S, Roberts AW, Metcalf D, et al. Hematopoietic stem cell

- deficiencies in mice lacking c-Mpl, the receptor for thrombopoietin. *Proc Natl Acad Sci U S A.* 1998;95(3):1195-1200.
46. Zheng C, Yang R, Han Z, et al. TPO-independent megakaryocytopoiesis. *Crit Rev Oncol Hematol.* 2008;65(3):212-222.
47. Machlus KR, Johnson KE, Kulenthirarajan R, et al. CCL5 derived from platelets increases megakaryocyte proplatelet formation. *Blood.* 2016;127(7):921-926.
48. Kanaji T, Vo MN, Kanaji S, et al. Tyrosyl-tRNA synthetase stimulates thrombopoietin-independent hematopoiesis accelerating recovery from thrombocytopenia. *Proc Natl Acad Sci U S A.* 2018;115(35):E8228-E8235.
49. Evstatiev R, Bukaty A, Jimenez K, et al. Iron deficiency alters megakaryopoiesis and platelet phenotype independent of thrombopoietin. *Am J Hematol.* 2014;89(5):524-529.
50. Chen S, Hu M, Shen M, et al. IGF-1 facilitates thrombopoiesis primarily through Akt activation. *Blood.* 2018;132(2):210-222.